

Real-time Continual Learning on Intel Loihi 2

Elvin Hajizada^{*1,2}, Danielle Rager¹, Timothy Shea¹, Leobardo Campos-Macias¹, Andreas Wild¹, Eyke Hüllermeier², Yulia Sandamirskaya³, and Mike Davies¹

¹*Intel Labs, Intel Corporation, Santa Clara, CA, USA*

²*Institute of Informatics, University of Munich (LMU), Munich, Germany*

³*Institute of Computational Life Sciences (ICLS), Zurich University of Applied Sciences (ZHAW), Wädenswil, Switzerland*

^{*}*Corresponding author: hajizada.elvin@campus.lmu.de*

Abstract

AI systems on edge devices face a critical challenge in open-world environments: adapting when data distributions shift and novel classes emerge. While offline training dominates current paradigms, online continual learning (OCL)—where models learn incrementally from non-stationary streams without catastrophic forgetting—remains challenging in power-constrained settings. We present a neuromorphic solution called CLP-SNN: a spiking neural network architecture for Continually Learning Prototypes and its implementation on Intel’s Loihi 2 chip. Our approach introduces three innovations: (1) event-driven and spatiotemporally sparse local learning, (2) a self-normalizing three-factor learning rule maintaining weight normalization, and (3) integrated neurogenesis and metaplasticity for capacity expansion and forgetting mitigation. On OpenLORIS few-shot learning experiments, CLP-SNN achieves accuracy competitive with replay methods while being rehearsal-free. CLP-SNN delivers transformative efficiency gains: 70x faster (0.33ms vs 23.2ms), and 5,600x more energy efficient (0.05mJ vs 281mJ) than the best alternative OCL on edge GPU. This demonstrates that co-designed brain-inspired algorithms and neuromorphic hardware can break traditional accuracy-efficiency trade-offs for future edge AI systems.

1 Introduction

A growing need in artificial intelligence is the deployment of physical edge AI systems such as service robots navigating cluttered homes and hospitals, autonomous drones monitoring ecosystems, and always-on health-monitoring wearables. These must operate in dynamic environments where lighting, background, or the set of relevant classes can change rapidly and unpredictably [37, 23, 43]. Neural networks are typically trained offline and deployed as static models. These models become restrictive when data is evolving or personalized, due to the closed-world assumption that training and deployment distributions remain identical [39]. In the open world setting, the accuracy of pretrained models degrades, making them inadequate for capturing the complexities of the real world over extended time-frames [50, 49, 53, 55]. Some scenarios allow for periodic model retraining and redeployment to address this [29, 38]. However, this approach is generally too slow and power-intensive for edge platforms [25]. Recent advances in large language and vision models offer an alternative approach to model retraining, known as in-context learning. However, these models require cloud-scale accelerators, gigabytes of memory, and must process hundreds of context tokens per adaptation, mak-

ing them impractical for energy-constrained edge devices [7].

Instead, models that adapt continuously to non-stationary data streams while operating within strict latency and memory budgets can run on edge devices. This paradigm, known as online continual learning (OCL), requires models to learn incrementally, while retaining prior knowledge with restrictions on data revisitability [41, 15, 5, 52]. This setting presents two core algorithmic challenges of the plasticity-stability dilemma [26]: (1) achieving targeted learning and accurate inference in the presence of continual distributional shifts, and (2) retention of previously acquired knowledge. The failure of retaining acquired knowledge, also known as catastrophic forgetting, leads the model to abruptly forget previously learned information when trained on new data [32]. Moreover, practical deployments may require few-shot adaptation to new situations from limited examples or detection and learning of novel concepts [24, 23, 6]. Yet, developing algorithms and hardware that robustly achieve these capabilities, especially under strict edge constraints, has been elusive so far.

Interestingly, biological brains have long faced and solved the same problems [27]. They learn continually using (i) metaplasticity mechanisms that stabilize memories [1, 4], (ii) neurogenesis and synaptic pruning that

expand capacity on demand [3], (iii) learning mechanisms that are local in both representation and weight adjustment [35, 30, 47], (iv) synaptic consolidation via memory replay [10, 18], and (v) asynchronous, event-driven communication [21]. When translated to engineering practice, these principles call for stateful neuron models to support metaplasticity, capacity for adaptive architectural growth, local learning rules, replay buffers, and asynchronous computation.

Spiking neural networks (SNNs) naturally meet these requirements: their event-driven spikes propagate information sparsely and asynchronously through stateful neurons [11], Hebbian-like plasticity rules implement local learning [54], and drop-and-grow mechanisms can add or remove neurons over time [17]. Neuromorphic processors such as Intel’s Loihi 2 exploit these properties in silicon, integrating memory and compute within each core, using sparse event-based communication, and executing learning rules only when and where spikes occur [9, 34, 42]. Loihi 2 also includes dedicated hardware acceleration for the online local learning algorithms [8, 12]. The combined effect of these features is orders-of-magnitude reductions in latency and energy compared to conventional CPU and GPU platforms [36, 9, 45].

Yet modern OCL algorithms are not designed for neuromorphic hardware. Most rely on large replay buffers to mitigate forgetting, overwhelming the limited on-chip (SRAM) memory available in edge devices and consuming additional energy each time past data are revisited [51]. Multi-task learning further overwhelms memory, as the replay buffer size grows proportional to the number of tasks [48]. Other methods employ dense gradient updates or covariance-matrix inversions that violate the locality assumption and slow down learning [2, 15]. Generally, the model throughput and latency of training are the crucial metrics that are rarely looked at for OCL scenarios [15]. All these challenges render current solutions impractical for edge AI deployment [40, 29] and highlight the importance of co-designing efficient algorithms and hardware [13, 31, 28].

Here we introduce an SNN extension of the Continually Learning Prototypes algorithm (CLP-SNN), which leverages brain-inspired principles while operating within the power and latency envelope of Loihi 2 [13]. CLP-SNN encodes knowledge locally in a number of class prototypes updated by a three-factor local learning rule; a metaplasticity mechanism consolidates mature prototypes to protect them from interference, while a neurogenesis module allocates new neurons on demand when the data stream contains unfamiliar concepts. Recently introduced as a replay-free OCL algorithm with few-shot and open-set learning capabilities, Continually Learning Prototypes (CLP) runs on conventional hardware [13]. Our CLP-SNN architecture and its neuromorphic implementation transform CLP into an edge-deployable, real-time, continual learning system. Evaluated against the CLP and other baseline algorithms

running on an edge GPU, CLP-SNN on Loihi 2 provides a reference for cross-platform benchmarking. In extensive experiments on the OpenLORIS robotic vision benchmark [44], CLP-SNN matches or exceeds the accuracy of replay and non-replay baselines while reducing per-sample learning latency and energy by orders of magnitude – thereby demonstrating that co-designed brain-inspired algorithms and hardware can indeed deliver real-time adaptation on the edge.

Recent comprehensive surveys have extensively reviewed the neuromorphic continual learning landscape, highlighting both unique advantages and persistent challenges [34, 33]. While substantial theoretical work exists on continual learning with SNNs, implementations on actual neuromorphic hardware remain rare, making our contribution particularly valuable for bridging this gap between theory and practice. Previous work on Loihi 1 established important precedents for on-chip learning implementations: Imam and Cleland [19] employed neurogenesis for continual odor learning, Hajizada et al. [12] designed neural state machines for object learning, and Stewart et al. [46] proposed SOEL for few-shot gesture recognition. Our work builds upon these foundations while introducing novel algorithmic components and demonstrating superior performance metrics on the more advanced Loihi 2 platform. The scarcity of comprehensive benchmarking between neuromorphic and conventional platforms represents a significant gap in the literature that our work addresses. By providing direct comparisons across accuracy, latency, and energy metrics, we establish a methodological framework for future neuromorphic continual learning evaluations.

Our specific contributions are: (1) a principled OCL framework grounded in locality, asynchrony, metaplasticity and growth aiming for real-time learning at the edge; (2) a new SNN architecture and self-normalising three-factor rule¹ together with an instantiation on a neuromorphic hardware; (3) a cross-platform benchmarking between Loihi 2 and an edge GPU; and (4) an empirical derivation of hardware requirements for real-time continual learning under tight latency and power budgets. To foster research in this field, we have open-sourced the simulated SNN code on the Lava framework [20], making it accessible to the broader research community. The remainder of the paper details the algorithm, its neuromorphic implementation, and the consequent system-level evaluation.

2 Results

CLP-SNN and its Loihi 2 implementation

Continually Learning Prototypes (CLP) is a comprehensive method for Open-World Continual Learning (OWCL) with capabilities supporting online continual learning, few-shot learning, novelty detection,

¹a learning rule that maintains weight norms without explicit normalization steps

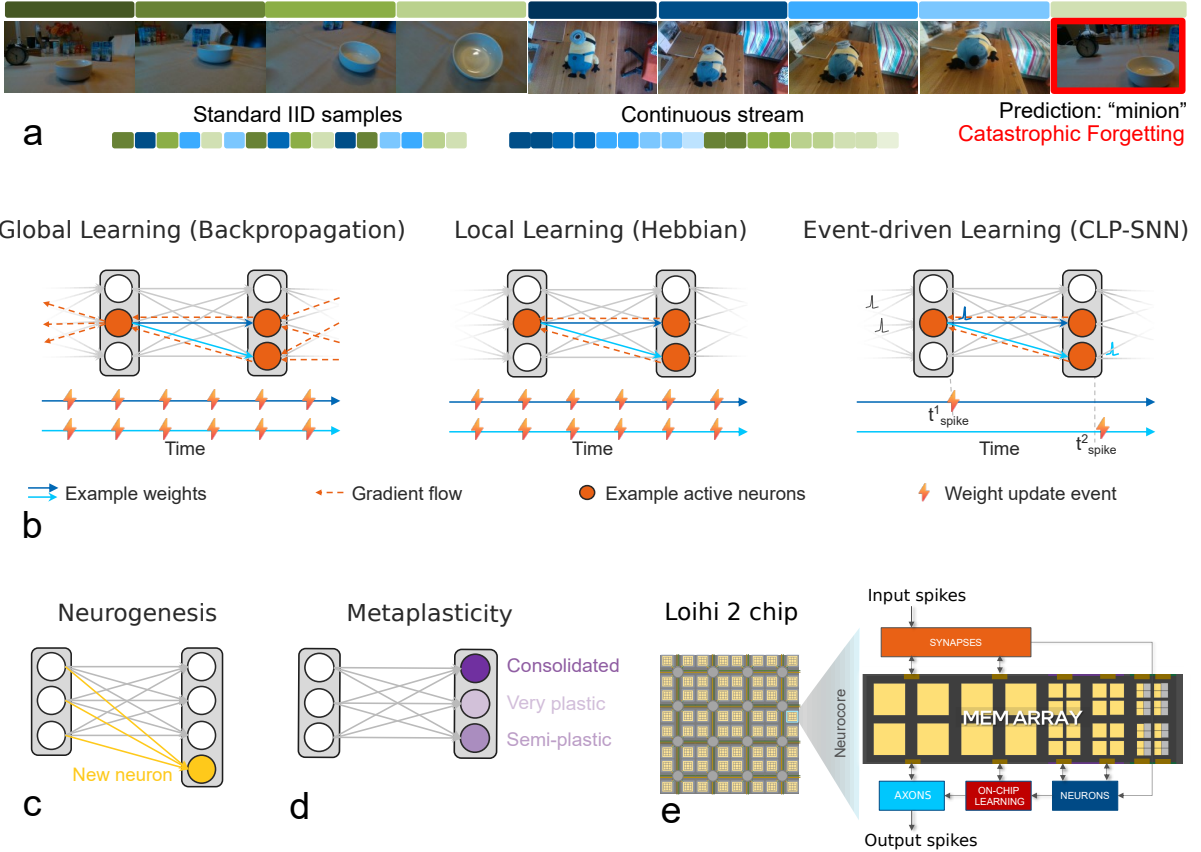


Figure 1: From dense global updates to event-driven local learning on neuromorphic chip Loihi 2, as an efficient solution to online continual learning. **a** Catastrophic forgetting happens when learning tasks (e.g. objects) are presented sequentially in non-i.i.d data streams. Online Continual Learning (OCL) is such a setting, where inference and learning occur per sample. **b** (Left) Global learning with backpropagation relies on non-local error signals (orange dashed arrows) and updates all weights every step (orange flashes), shown only for two example weights (blue arrows). This produces spatially and temporally dense learning, which is inefficient. (Middle) Local Hebbian learning relies solely on local information, making it more efficient; however, it is enacted at each timestep for all neurons, remaining spatially and temporally dense. (Right) Event-driven local learning triggers weight updates only when and where spikes occur (e.g., at t^1_{spike} for the first weight and t^2_{spike} for the second weight), resulting in spatially and temporally sparse updates that facilitate efficient and rapid learning. To achieve such learning, CLP-SNN employs a 3-factor local learning rule triggered by a selective modulatory signal. **c** CLP-SNN proposes a neurogenesis mechanism to increase capacity on demand as new concepts are learned, and **d** metaplasticity, which modulates plasticity over time (from very plastic to consolidated) to address catastrophic forgetting. **e** Intel Loihi 2 neuromorphic chip with neurocores supporting on-chip, event-driven communication across axons, neurons, and synapses, enables local, sparse learning.

and semi-supervised learning [13]. At its core, CLP stores representative samples or *prototypes* to capture the prototypical representation of classes in feature space (Fig. 2b). CLP adjusts these prototypes dynamically based on sparsely labeled streaming input. The learning process is semi-supervised: if a sample is labeled, CLP uses its label to make a more precise update. Otherwise, it behaves as an unsupervised clustering algorithm. CLP’s novel metaplasticity mechanism tackles catastrophic forgetting, in that each prototype’s plasticity (learning rate) is adjusted based on the correctness of inference (Fig. 1d). It allocates new prototypes on demand for each new concept captured through a novelty detection mechanism. Thus, CLP builds a multi-prototype representation for each class with a varying number of prototypes. Importantly, CLP does not require rehearsals

or a memory buffer to address catastrophic forgetting.

We designed a spiking neural network (SNN) architecture for the CLP algorithm, called CLP-SNN (Fig. 2), and contributed the following: (1) a novel self-regularizing local learning rule, (2) a neural state machine with programmable neurons to achieve spatiotemporally sparse event-driven weight updates, and (3) implementation in the Loihi 2 chip (Fig. 1e) to demonstrate an efficient neuromorphic learning system.

In our SNN architecture, we modeled prototypes as neurons storing each prototype vector in the prototype neuron’s input weights (Fig. 2a-b). We utilize dot product similarity to assign inputs to prototypes, as in the CLP algorithm, assuming that all input vectors and weight vectors are L2-normalized [13]. Thus, the activation accumulated in each prototype neuron, that amounts

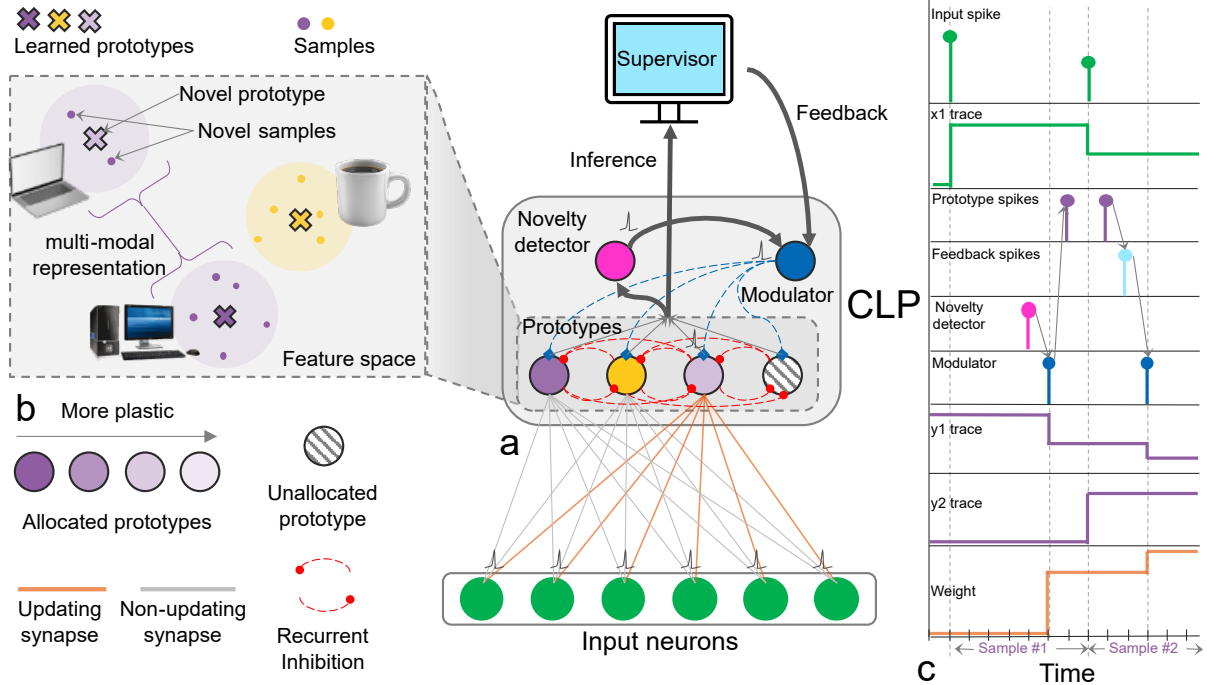


Figure 2: The proposed spiking neural network (SNN) architecture for the CLP algorithm. **a** The SNN consists of multiple neural populations, where the prototype neurons are central. Each prototype neuron has its plasticity level that controls the scale of the update applied to its input synapses. The prototypes compete using a winner-take-all mechanism implemented through lateral inhibition. For each sample, only one (winner) prototype neuron updates its weights. If no neuron spikes, the input sample is detected as novel by a novelty detector neuron, which triggers a modulator neuron, which in turn triggers learning in one of the unallocated prototype neurons. If there was a winning neuron, its label is considered the inferred label, and the supervisor sends a feedback signal based on the correctness of this inference. This is relayed to the prototype population via the modulator neuron to update the respective prototype neuron. **b** A pictographic view of the feature space and representation of the prototypes in this space. Each class may have a variable number of prototype neurons. **c** Temporal dynamics of inference, novelty detection, feedback, and learning in SNN time step resolution. The first sample of "laptop" triggers the allocation of a new (transparent) purple prototype neuron, while the second sample updates this neuron's synapses further. The dynamics are depicted for one of this neuron's input synapses over the time for processing of two samples.

to the dot product between input and input weights, is equivalent to cosine similarity between the input and the prototypes. These activations are translated into a spike if they exceed a threshold, with the spike timing that depends on the activation level. Hence, CLP-SNN identifies the winning prototype by detecting the earliest spike. It also implements a winner-take-all (WTA) mechanism using lateral inhibition among prototype neurons to keep a single winner neuron. CLP-SNN sends this output to a *supervisor* as its prediction for evaluation (Fig. 2a). The outputs of the prototype neurons are also sent to a *novelty detection neuron*. If this neuron does not record any spike during a set delay period after input injection, it will eject a spike signaling novelty detection (Fig. 2c). This, in turn, activates a *modulator neuron*, which sends a feedback spike to the prototype neuron population as a modulatory (third-factor) signal. One of the prototype neurons, which has not yet learned any pattern, is forced to spike and learns the input pattern as a new prototype (Fig. 2c).

The *modulator neuron* also receives a positive or negative feedback signal from the *supervisor*, based on comparison of the output and the actual label. It relays this

signal to the winner prototype neuron in the form of a third-factor spike, as that prototype neuron decides the network's output. This supervisory signal is optional, and in its absence the *modulator neuron* nevertheless sends a positive spike to perform unsupervised learning. In this paper, we focus on the supervised paradigm and refer the reader to the CLP paper [13] for the unsupervised learning experiments.

For each sample, only the winner prototype neuron that spiked first updates its input weights and individual dynamic learning rate (i.e., plasticity) based on this third-factor spike. The scale of each update depends on the internal learning rate, represented by a dynamic neuron parameter. The fine-grained nature of the winner neuron's plasticity thus implements the metaplasticity mechanism to mitigate forgetting. Subsequently, we propose the following learning rule to modify the input weights of the prototypes:

$$\mathbf{w}_{n+1}^{(k)} \leftarrow \mathbf{w}_n^{(k)} + \alpha_n^{(k)} r_n^{(k)} (\mathbf{x}_n - \mathbf{w}_n^{(k)} y_n^{(k)}), \quad (1)$$

$$y_n^{(k)} = \mathbf{w}_n^{(k)T} \mathbf{x}_n, \quad (2)$$

where at the time of processing n -th sample, $\mathbf{x}_n \in \mathbb{R}^d$ is

the d -dimensional input vector, $\mathbf{w}_n^{(k)} \in \mathbb{R}^d$ is the weight vector, $\alpha_n^{(k)} \in [0, 1] \subset \mathbb{R}$ is the learning rate (i.e. plasticity), $y_n^{(k)} \in [-1, 1] \subset \mathbb{R}$ is the post-synaptic activation of the prototype k . Importantly, $r_n^{(k)} \in [-1, 0, 1]$ is the third-factor feedback signal arriving at the prototype neuron k , and $r_n^{(k)} = 0$ for all prototypes, except the winner prototype. This enables spatiotemporal weight update sparsity by selecting when and which prototype neuron to update (Fig 1b-right). We can also write the learning rule for the input weight vector of the winner prototype neuron for the n -th sample as follows:

$$\Delta \mathbf{w} = \alpha_n r_n (\mathbf{x}_n - \mathbf{w}_n y_n), \quad (3)$$

where $r_n^{(k)} \in [-1, 1]$. Also note that the time steps $n, n+1, \dots$ are the algorithmic time steps, each corresponding to inference and learning of a single sample. In each such step, multiple SNN time steps pass to produce temporal coded prototype spikes, modulatory, and feedback spikes (see Sec. 4 for more details).

Loihi 2 implementation for CLP-SNN. We leverage Loihi’s hardware-level learning acceleration and other features to build an efficient implementation of CLP-SNN. The three-factor local plasticity rules of Loihi 2 enable event-driven, targeted, and sparse weight updates (Fig. 1e). CLP-SNN’s learning rule (equation (3)) is a good fit for Loihi 2, as it incorporates pre- and post-synaptic activity modulated by a third-factor signal. The adaptive learning rates and goodness scores appearing in the learning rule are stored as the internal variables of prototype neurons, which the HW-level learning acceleration can access. We also leverage other features of Loihi 2: programmable neurons to design complex neuronal behaviors, integer-valued spikes for more efficient communication among neurons compared to binary spikes, and input-dependent maintenance of the pre-synaptic traces.

Self-normalizing learning rule of CLP-SNN

At a closer look, the similarity of CLP-SNN’s learning rule to Oja’s rule [35] is evident: α_n and r_n can be aggregated into a single learning rate term, and then only the scaling by the post-synaptic activation seems absent. This similarity to Oja’s rule is not coincidental. Oja’s rule is a modification of the basic Hebb rule [16], where the weights are continuously normalized through multiplicative normalization to avoid indefinite growth of weights. The original CLP learning rule has no internal normalization mechanism, as the algorithm performs explicit normalization of the weight vectors after each learning update. Therefore, the original CLP learning rule for the n -th sample looks like as follows in our notation:

$$\Delta \mathbf{w}_{CLP} = \alpha_n r_n \mathbf{x}_n. \quad (4)$$

However, explicit normalization requires global operations that compute vector norms and apply normalization

across all synaptic weights simultaneously. Such operations are biologically implausible, as biological neurons lack the machinery to perform global normalization operations that depend on the weights of all synapses. The same constraints apply to neuromorphic chips like Loihi 2: global normalization operations would require collecting synaptic weights from distributed memory locations, computing norms centrally, and rewriting the normalized values back, thereby violating the principle of locality and negating the energy and latency advantages of neuromorphic architectures.

Therefore, while designing the SNN architecture for CLP, we began with the original CLP learning rule and employed a methodology similar to the derivation of Oja’s rule to derive a modified learning rule that implicitly normalizes the weights. Our approach utilizes Taylor expansion and assumes a small learning rate to derive this new learning rule. The detailed derivation is provided in the Methods section. The design and derivation of the learning rule represent one of the core contributions of this paper.

CLP-SNN outperforms rehearsal and non-rehearsal methods under few-shot streaming setting

In this paper, we focus on the supervised few-shot online continual learning experiments and refer the reader to the original CLP paper [13] for novelty detection and semi-supervised experiment results. We employed the same setup involving the OpenLORIS dataset [44] as in the original CLP paper: single pass over non-shuffled frames of 40 classes, which are pre-processed by a fixed pre-trained feature extractor (Fig 1a). The goal for the OCL algorithm here is to learn objects from such streams while avoiding catastrophic forgetting of the learned objects. In the one-shot setting, a single short video clip per object category is sequentially injected into the OCL model.

In the one-shot setting, we trained CLP, CLP-SNN (on Loihi 2), and competing algorithms² [15, 13] on a sequence of 40 online learning tasks, each containing a single short video clip per object category, similar to class-incremental learning. In addition to the final accuracy, we are also interested in the evolution of accuracy during the learning process over previously learned classes. Therefore, after each learning task, we test on all seen tasks (i.e., classes) to measure the online accuracy of the model. We repeated this experiment for three different random orders of classes. Fig. 3a shows the accuracy trends for all methods over these class-incremental learning tasks. Both CLP and CLP-SNN outperform other methods. The gradual decrease in the accuracy is the result of the classification task getting inherently harder as more classes are added. We also observe that non-CL baselines (fine-tuning and perceptron) are significantly worse than OCL methods, hinting at the catastrophic

²We used the implementations from [Embedded-CL repo](#) by Tyler Hayes for the baseline methods.

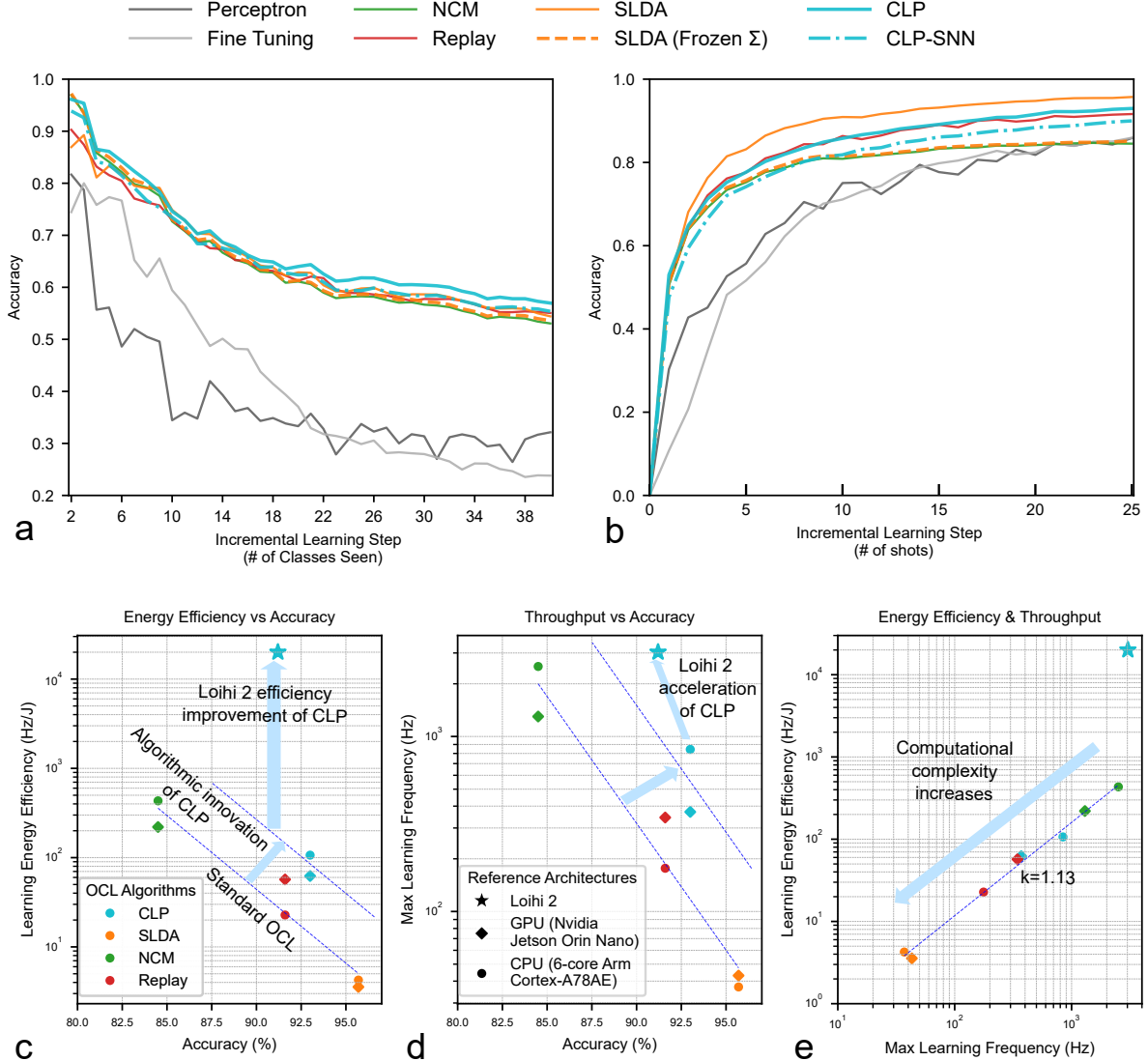


Figure 3: Few-shot online continual learning experiments with OpenLORIS dataset. **a** The comparison of the trends for average accuracy rate on observed classes during the 1-shot learning experiment. While offline learning methods (grays) fail, OCL algorithms retain accuracy, and CLP outperforms the baselines. The gradual decay of accuracy is a result of the increase in task difficulty (more classes to differentiate among). **b** 25-shot OCL experiment. Each time step corresponds to one shot. CLP outperforms all methods except SLDA, which, thanks to its use of the covariance matrix, can leverage the data better, albeit with higher latency and energy costs (see Table 1). In both experiments, CLP-SNN slightly underperforms CLP, as a result of the weight/activation quantization and discretized temporal WTA. **c** Energy efficiency versus accuracy trade-offs for online continual learning algorithms across different hardware architectures. Accuracy values are recorded at the end of 25-shot learning experiment. The dashed diagonal line represents the standard OCL performance boundary in conventional computing architectures. CLP on the GPU/CPU already improves this boundary thanks to its algorithmic innovations, such as multi-prototype learning and adaptive learning rates. This is further improved significantly ($\sim 200\times$) by Loihi 2 implementation. **d** The learning throughput versus accuracy trade-off yields results similar to the other (c) trade-off. **e** Learning throughput versus energy efficiency.

forgetting of non-CL methods. CLP-SNN has a slight accuracy drop compared to CLP, resulting from INT7 weight/activation quantization and discretized temporal WTA. Nevertheless, it still achieves higher accuracy in this low-data setting.

CLP-SNN improves accuracy-latency-energy trade-off

While results from the previous experiments are encouraging, further investigation of the long-term stability of all competing methods is necessary. Specifically, we provide 25 subsequent learning shots to the models, with each shot including one video for each object—totaling 40 videos per shot. The rest of the experimental setup

Table 1: Performance comparison table.

Method	System	Quantization	Acc (%) (1-shot)	Acc (%) (25-shot)	Latency (ms)	Total energy (mJ)	Dynamic energy (mJ)	Total EDP (μ Js)
CLP	Loihi 2 ¹	INT7	<u>55.4</u>	90.0	0.33	0.05	0.01	0.02
	GPU ²	FP32	57.0	<u>93.0</u>	2.70	16.07	2.66	43.34
	CPU ³	FP32	57.0	<u>93.0</u>	1.19	9.38	3.45	11.12
NCM	GPU	FP32	53.1	84.5	0.77	4.54	0.72	3.49
	CPU	FP32	53.1	84.5	<u>0.40</u>	<u>2.31</u>	<u>0.34</u>	<u>0.92</u>
Replay	GPU	FP32	55.1	91.6	2.90	17.55	3.13	50.98
	CPU	FP32	55.1	91.6	5.66	43.94	15.65	248.2
SLDA	GPU	FP32	54.4	95.7	23.2	281	162	6528
	CPU	FP32	54.4	95.7	26.9	235	99	6352

¹ Loihi 2 Oheo Gulch system with N3C2-revision chips running on Lava 0.11.0.dev0, Lava-Loihi 0.6.0.dev0 and NxCore 2.5.8.

² NVIDIA Jetson Orin Nano 8GB (15W TDP) running PyTorch 2.4.0. Energy values include *CPU*, *GPU*, *CV* and SOC components.

³ NVIDIA Jetson Orin Nano’s 6-core Arm Cortex-A78AE CPU

is the same as the previous experiment: no shuffling of video frames and a single pass over the data. This allows us to test the models under domain shifts, similar to a domain-incremental setting, as no new class is introduced after the first shot.

Over the learning period, we observe that the methods start to differentiate more in terms of accuracy, as CLP surpasses both NCM and Replay, while CLP-SNN has accuracy slightly lower than CLP (Fig. 3d). NCM can be considered the simplest form of CLP, as it uses only one running average prototype for each class, resulting in much less modeling power than CLP. Clearly, CLP’s adaptive multi-prototype per-class model leverages the extra data. By surpassing the Replay method, CLP also demonstrates that rehearsal-free CL can achieve performance comparable to rehearsal-based methods. Conversely, SLDA slightly outperforms CLP, attributable to its extra modeling capabilities and online covariance matrix update mechanism. This heavy matrix inversion operation is performed before every intermediate evaluation, which in our case is after learning a single video (60 frames). Importantly, SLDA with a frozen covariance matrix performs only as well as NCM, and the adaptive SLDA achieves this marginal accuracy improvement at a huge cost of latency and energy consumption.

Subsequently, we compared the Loihi 2 implementation of CLP-SNN against its OCL competitors, running on the Jetson Orin Nano GPU (Table 1). CLP-SNN improves latency by 70 \times (0.33ms vs 23.2ms) and energy consumption by 5,600 \times (0.05mJ vs 281mJ) per learning update as compared to the standard FP32 SLDA implementation on Jetson Orin Nano GPU (Table 1). Even when compared to NCM, the simplest conventional OCL method, CLP-SNN, still demonstrates 51 \times EDP and 1.2 \times latency gains, while surpassing NCM accuracy by 7%. CLP-SNN is also vastly more efficient (1000 \times EDP and 4 \times latency improvement) than the FP32 CPU/GPU reference implementation of CLP. This energy-latency-accuracy trade-off is visualized in Fig. 3c,d,e. As shown in Fig. 3, other OCL algorithms fall onto clear trade-off

frontier lines: better performing methods have lower energy efficiency (Fig. 3c) and lower learning frequency, i.e., higher latency (Fig. 3d). In both figures, CLP on conventional hardware already improves the frontiers and achieves the same accuracy with higher energy efficiency and at a higher frequency, demonstrating the value of CLP’s algorithmic innovations. Loihi 2 implementation of CLP (CLP-SNN) further accelerates the algorithm and improves efficiency, showcasing the value of Loihi 2, neuromorphic implementations of CLP and in general learning. Our benchmark results use buffered inputs for learning, excluding I/O between the host and device, both for GPU and Loihi. While we suspect that using ONNX or TensorRT runtime optimizations may reduce the latency of GPU solutions, we do not expect these optimizations to eliminate CLP-SNN’s large EDP or latency advantage.

Sparsity matters, but not all sparsity types are created equally

We also characterized the latency and energy for CLP-SNN under different conditions. The most performant and efficient setting exploits two types of sparsity: (1) input sparsity, where the feature vectors are sparse, and (2) temporal sparsity of learning. In our characterization experiments, we apply 50% sparsity for input features, which is the average sparsity of the feature vectors extracted from OpenLORIS, and for temporal sparsity of learning, we use t_{epoch} of 20 time steps (ts), meaning learning happens once every 20 ts, which is required time to process a sample. We did ablation studies of this most performant setup, investigating how performance changes, e.g., when the input is dense, or learning is applied every time step, etc. These ablation studies yielded several concrete insights. Firstly, input sparsity brings a significant speed-up for the non-learning components (spiking phase) of processing: 50% sparsity creates 28% decrease in spiking phase latency. Secondly, temporal sparsity of the learning, i.e., only intermittently execut-

ing the learning rule, is critical to speed up processing. The learning phase latency is inversely proportional to the t_{epoch} parameter. CLP-SNN runs 20 times faster when t_{epoch} is increased from 1 to 20. Respectively, dynamic power consumption is 3.5 times less. Thirdly, the spiking phase dominates the execution time of CLP-SNN if t_{epoch} is large. However, it is dominated by the learning phase if t_{epoch} is near to one. Finally, if learning is enabled for a neuron, the latency and power cost of the learning phase for this neuron is not affected by post-synaptic gating of the learning rule. This means that if the learning rule depends on the post-synaptic spike (i.e. y_0), there is no significant difference between the presence or absence of this gate, in terms of computational cost, as most of the learning engine computations are independent of this gating.

Online continual learning methods are resource-intensive and can benefit from specialized computing architectures

One important insight from the latency and energy benchmarking is that online, continual learning methods are very resource-intensive, even though they are based on single-layer networks. The dynamic energy consumed during learning is a good measurement for the computational load of these methods. The other component of the total energy, i.e., static one, is more hardware specific, and other parallel workloads may run in the same system during actual deployment. When implemented on the same hardware (on NVIDIA Jetson Orin Nano), SLDA consumes $480\times$ more dynamic energy, compared to NCM. This demonstrates that SLDA is a computationally heavy algorithm, especially when the input feature dimensionality is high (1280-d in this case) and the covariance matrix (1280x1280) is updated periodically. In Fig. 3f, we observe that CLP-SNN on Loihi 2 breaks out from the frontier of the methods running in conventional HW. This boundary has a slope of 1.13 in the log-log plot, meaning energy efficiency gets super-linearly worse as the latency increases, while the computational load of the methods increases. This boundary includes CLP’s CPU/GPU implementation too, and clearly, a novel HW like Loihi 2 can break this frontier.

3 Discussion

The capabilities of modern deep learning-based AI systems are impressive. While these are adequate for applications with stationary task parameters, some current and future use cases will require real-time adaptive intelligence. Therefore, OCL is positioned to complement the current training paradigms by facilitating short- and long-term adaptivity from non-stationary data streams, while avoiding catastrophic forgetting. Moreover, low latency and energy efficiency are critical but overlooked requirements. Neuromorphic systems and spiking neural networks (SNNs), inspired by biological

neural computation, naturally align with OCL requirements through their event-driven, sparse, and local learning mechanisms. Their inherent low-power, low-latency computation capabilities make them well-suited for edge applications where traditional deep learning approaches become impractical due to resource constraints.

The primary contribution of our work lies in demonstrating a holistic approach to adaptive real-world edge AI systems that addresses multiple challenges simultaneously. CLP-SNN not only mitigates catastrophic forgetting while learning from non-i.i.d. data streams but also provides a practical hardware implementation that enables real-time, energy-efficient learning. Our approach represents the first continual learning implementation on Loihi 2, establishing new performance benchmarks for neuromorphic continual learning.

The CLP-SNN architecture achieves its advanced performance by several key algorithmic innovations: (1) an event-driven neural state machine that enables spatiotemporally sparse weight updates, (2) a novel self-normalizing three-factor learning rule that eliminates the need for explicit weight normalization, and (3) neuronal implementation of the biologically-inspired mechanisms including metaplasticity for catastrophic forgetting mitigation and neurogenesis for adaptive capacity expansion. We also implemented an instantiation of CLP-SNN on the Loihi 2 neuromorphic chip. Our cross-platform benchmarking provides valuable insights for future edge hardware architectures for efficient real-time learning.

These innovations collectively demonstrated that co-designed brain-inspired algorithms and specialized hardware can deliver substantial improvements over conventional approaches across the critical metrics of accuracy, latency, and energy consumption. The CLP algorithm improves upon conventional OCL methods, as evidenced by breaking from the Pareto frontier of the baseline methods, even when implemented on conventional hardware. The neuromorphic implementation on Loihi 2 amplifies these advantages by exploiting the alignment between brain-inspired architecture of CLP-SNN and neuromorphic computing principles. Our results show that CLP-SNN achieves $70\times$ latency improvement and $5,600\times$ energy efficiency gains compared to the best-performing baseline OCL method, while maintaining comparable or superior accuracy. These improvements stem from the event-driven nature of spike-based computation and weight updates, the locality of learning rules that minimize data movement, and the integration of memory and computation that reduces the traditional von Neumann bottleneck. The spatial and temporal sparsity characteristics of our approach provide important insights for future neuromorphic system design. While input sparsity (50%) resulted in meaningful latency reductions (28%), temporal sparsity of learning proved even more critical, with $20\times$ improvements when learning occurs every 20 timesteps rather than continuously.

While the Loihi 2 instantiation of the CLP-SNN architecture exhibits impressive performance, it has limita-

tions. The current implementation employs a simplified prototype allocation strategy where prototypes are assigned after novelty detection but this assignment is not subsequently adapted. Although this approach maintains the core learning capabilities, energy, and latency advantages demonstrated in our benchmarking, it requires 2-3× more prototypes compared to a fully adaptive CLP-SNN, which currently runs in a simulated version of the algorithm. Importantly, the energy and latency gains will hold for a fully adaptive CLP-SNN implementation on Loihi 2, as the computational load of a single weight update remains the same in both cases.

The reliance on fixed feature extractors represents another limitation inherent to shallow continual learning approaches. While this constraint affects all competing methods in our evaluation, complex learning scenarios with substantial domain shifts may require continual adaptation of feature representations. We identify the synergistic continual update of both CLP mechanisms and feature extractors as a promising direction for future research.

Our hardware characterization provides valuable insights for next-generation neuromorphic architecture design. Similar to other reports in the literature [45], we observed that sparse communication facilitated by input sparsity speeds up inference. Regarding learning, our experiments demonstrated that the event-driven nature of learning brings significant gains in learning latency.

While the temporal sparsity of learning evidently improves latency, we did not observe similar gains for spatial sparsity of learning on Loihi 2. Updating a single neuron’s weight did not improve latency compared to updating multiple neurons’ weights. This originates from the current design of the on-chip learning acceleration of the Loihi 2. The limitation relates to post-synaptic gating of learning execution: the effect of such gating comes late into the picture, hence the computational cost of the learning already occurred by the time of the gating function. On the other hand, pre-synaptic gating has a more significant positive effect on latency, as it gates learning execution earlier. Hence, we think future on-chip learning acceleration should prioritize strict conditioning on all gating events (pre-synaptic, post-synaptic, and third-factor) to support spatiotemporally sparse learning.

Overall, our results represent a fundamental shift in the feasibility of deploying continual learning systems in resource-constrained environments, opening new possibilities for autonomous vehicles navigating changing environments, medical devices personalized to individual patients, and IoT sensors adapting to seasonal variations. From a sustainability perspective, the substantial improvements of energy efficiency of neuromorphic continual learning could significantly reduce the carbon footprint of AI systems, particularly those deployed at scale across edge networks.

4 Methods

Derivation of CLP-SNN Rule

In this section we will derive our CLP-SNN learning rule from the original CLP rule [13], which is:

$$\Delta \mathbf{w} = \alpha \mathbf{r} \mathbf{x}.$$

Note that we can combine $r \in \{-1, 0, 1\}$ term into α , as it is just the sign of the modulatory signal. After applying CLP learning, the new weight is:

$$\mathbf{w}^{\text{new}} = \mathbf{w} + \alpha \mathbf{x}$$

To be able to perform cosine similarity between the input and the weight vector, in CLP algorithm, the weight vector is re-normalized after each update:

$$\mathbf{w}^{\text{new}} = \frac{\mathbf{w} + \alpha \mathbf{x}}{\|\mathbf{w} + \alpha \mathbf{x}\|}$$

and for the i -th component:

$$w_i^{\text{new}} = \frac{w_i + \alpha x_i}{\sqrt{\sum_j (w_j + \alpha x_j)^2}}$$

Next, we expand the denominator:

$$\begin{aligned} \sum_j (w_j + \alpha x_j)^2 &= \sum_j w_j^2 + 2\alpha \sum_j w_j x_j + \alpha^2 \sum_j x_j^2 \\ &= 1 + 2\alpha y + \alpha^2 \end{aligned}$$

assuming the current weight and the input vectors are normalized, i.e., $\sum_j w_j^2 = 1$, $\sum_j x_j^2 = 1$, and where $\sum_j w_j x_j = \mathbf{w}^\top \mathbf{x} = y$. Therefore, the denominator now is:

$$\sqrt{1 + 2\alpha y + \alpha^2}$$

We can apply the Taylor expansion for $\sqrt{1+u}$ around $u = 0$:

$$\sqrt{1+u} \approx 1 + \frac{u}{2} - \frac{u^2}{8} + O(u^3)$$

Let’s now set $u = 2\alpha y + \alpha^2$,

$$\sqrt{1 + 2\alpha y + \alpha^2} \approx 1 + \alpha y + O(\alpha^2)$$

We can drop $O(\alpha^2)$ for $\alpha \ll 1$. Substituting the expansion, the normalized weight update is:

$$w_i^{\text{new}} = \frac{w_i + \alpha x_i}{1 + \alpha y}$$

We can use the first-order approximation $(1 + \epsilon)^{-1} \approx 1 - \epsilon$ for small ϵ , based on fact that $y \leq 1$ for cosine similarity and assuming again that $\alpha \ll 1$:

$$w_i^{\text{new}} \approx (w_i + \alpha x_i)(1 - \alpha y)$$

Expanding terms:

$$w_i^{\text{new}} \approx w_i + \alpha x_i - \alpha y w_i + O(\alpha^2)$$

After dropping $O(\alpha^2)$ term for small learning rates, we arrive at final CLP-SNN learning rule:

$$\Delta w_i = \alpha x_i - \alpha y w_i = \alpha(x_i - w_i y)$$

Note that this is a local learning rule depending only on the weight, pre- and post-synaptic activations. This is also the same learning rule as in equation (3), except for the vector notation and the missing third-factor term r , which can be easily added, as it only affects the sign and sparsity of the updates:

$$\Delta \mathbf{w} = \alpha r(\mathbf{x} - \mathbf{w}\mathbf{y})$$

Overall, the learning rule can be interpreted as follows:

- The term αx_i pushes the weight vector (i.e., the prototype) towards or away from the input, based on the correctness of the prediction.
- The decay term $-\alpha y w_i$ acts as an implicit normalization, preventing unbounded growth of the weights and maintaining their norm. This way, the simple dot product between the input and the weight vector will always be equivalent to the cosine similarity measure.
- $O(\alpha^2)$ collects all terms of second order and higher in α , which are negligible for sufficiently small learning rates. The initial imprinting of the weights by the normalized input vector after the novelty detection and prototype allocation guarantees that the initial weight will be normalized. Further updates need to adhere to the small learning rate assumption to keep the weights approximately normalized.

Details of the CLP-SNN architecture

We designed a spiking neural network comprising four key populations (Fig. 2b):

1. **Input Population:** Encodes feature vectors as integer-valued spikes, and synchronous spike emission represents one sample
2. **Prototype Population:** Each neuron stores one prototype as input weights, employs winner-take-all competition via lateral inhibition, and stores adaptive learning rates stored as internal parameters.
3. **Novelty Detector Neurons:** Triggers when no prototype spikes within window, using timer-based mechanism
4. **Modulator Neuron:** Converts external feedback and novelty allocation signal to third-factor signals, achieving sparse learning updates

In the CLP-SNN architecture and throughout this paper, we use two distinct notions of time:

1. **Algorithmic time step (n):** One step corresponds to the arrival and processing of a new sample (e.g., an input feature vector). Each algorithmic time step entails a full cycle: inference, novelty detection, feedback, and learning events for a single training example.
2. **SNN time step (t):** The smallest discrete time unit used in the simulation and hardware. All spiking neuron dynamics, including membrane potential integration and spike emission, evolve at this scale.

For each algorithmic time step (n), many SNN time steps (t) may occur. Specifically, the system processes the input over several SNN time steps until all the relevant spikes, competition, and learning events for that sample are complete. Only when this episode finishes do we increment n and present the next sample. Unless otherwise stated, each " n " step consists of 20 " t " time steps and equations involving n pertain to the higher-level algorithmic loop (e.g., weight updates per sample), while variables indexed by t capture state within the finer-grained spiking simulation (e.g., traces, spike trains).

The prototype population finds the best-matching prototype using a winner-take-all competition implemented via all-to-all lateral inhibitory connections. Once the winning prototype neuron spikes, it goes to all prototypes, including itself, to inhibit any further spike activity. The third-factor spike the prototype k receives ($r_n^{(k)}$ in equation (3)) can be either a negative or positive third-factor spike, signaling the punishment or reward for the winner prototype neuron. If the signal is negative, the weight vector of this neuron is pushed away from the input vector to decrease similarity, and, if positive, vice versa. Overall, the third-factor spike r_k^n imparts prototype selectivity to weight updates.

The modulatory signal $r_i^{(n)}$ implements a context-dependent learning gate that determines when and how synaptic updates occur. Rather than a complex conditional equation, we describe its behavior through the following biological-inspired logic:

Competition, Inference and Novelty Detection: During each algorithmic time step n , prototype neurons compete via winner-take-all dynamics. The winning neuron k^* is determined by:

$$k^* = \arg \max_i y_n^{(k)}, \quad \text{subject to } y_n^{(k^*)} > \theta$$

in which θ is a fixed threshold below which all prototype neurons are considered "inactive". If there is a winner prototype, it generates an output spike, and this prototype's assigned class label is interpreted as the prediction of CLP-SNN by the supervisor. If none of the prototypes pass the threshold, then none of the prototypes spike, and, in this case, the novelty detection neuron signals the detection of a novel pattern via a spike that identifies the next neuron to allocate. For this purpose, the novelty detector neuron keeps track of the next unallocated neuron. This spike arrives at the modulatory neuron to be relayed

to the prototype neuron population as the adequate third-factor spike to trigger imprinting of the inputs into the weight of the new prototype neuron. Subsequently, the label of the pattern is assigned to this newly allocated prototype.

Modulatory Signal Assignment: The third factor for each neuron is then determined by:

$$r_n^{(k)} = \begin{cases} +1 & \text{if } k = k^* \text{ and prediction is correct} \\ -1 & \text{if } k = k^* \text{ and prediction is incorrect} \\ +1 & \text{if } y_n^{(k^*)} < \theta \text{ and } i \text{ is the next free neuron} \\ 0 & \text{otherwise} \end{cases} \quad (5)$$

The prediction is evaluated based on the output of the prototype population and the target label by the supervisor. This design ensures that:

- Only the winning prototype receives learning signals (spatial sparsity)
- Correct predictions are reinforced ($r_i = +1$)
- Incorrect predictions trigger corrective updates ($r_i = -1$)
- Novel inputs activate prototype allocation ($r_i = +1$ for the next unallocated neuron)
- Non-competing neurons remain unchanged ($r_i = 0$)

Hence the modulatory signal is generated by the neural state machine comprising the novelty detector neuron, the modulator neuron, and the supervisor, which collectively implement the contextual logic described above.

Weight Update: Subsequently, the learning rate of the winner neuron dictates the scaling of the weight update, and multiplicative normalization keeps the weight vector normalized. When designing the SNN architecture for CLP, we interpreted each prototype neuron's individual dynamic learning rate as an internal learnable parameter. By default, all neurons start with an initial learning rate of one, and their weights are initialized to zero. Therefore, when a neuron spikes for the first time, according to equation (3), its weights are updated to reflect the current input, meaning the neuron is now assigned to represent that input. At this initial update, exceeding the small learning rate assumption mentioned in Sec. 2 is permissible because the input is already normalized and consequently, imprinting the input onto the weights also ensures that the weights remain normalized. However, all subsequent updates to this neuron must be performed using relatively small learning rates to maintain the normalization of the weights. Our simulations suggest that a learning rate of $\alpha < 0.3$ strikes a good balance.

Learning Rate Update: As in CLP algorithm [13], our SNN architecture also adjusts the learning rate of the winning neuron based on its prediction accuracy. Specifically, the neuron's learning rate decreases when it makes

a correct prediction and increases when it makes an incorrect one. To facilitate this process, each prototype neuron has an additional internal state called *goodness* (g), which is incremented or decremented by one after each correct or incorrect prediction. The prediction accuracy for each sample can be identified using simple match-mismatch neuron circuitry, which receives the prediction from the network and the actual label. In the next section, we describe the mechanistic details of the CLP-SNN through its Loihi 2 implementation

Neuromorphic implementation of CLP-SNN on Loihi 2 chip

Intel Loihi 2 is a digital neuromorphic chip with 128 neurocores, each simulating up to one million neurons and 123 million synapses implemented with 32 KB of neuron SRAM and up to 128 KB of synapse SRAM per core [36, 45]. Each neurocore supports up to 8192 neurons, with custom microcode-programmable neuron models, and dense, sparse, or convolutional weights. SRAM memory banks of different sizes can be flexibly partitioned among the neurons, offering different trade-offs between energy, bandwidth, and capacity. Loihi 2 operates with asynchronous communication on sub-timestep granularity, while using barrier synchronization per timestep, resulting in algorithmic timesteps with varying lengths depending on the computational load incurred during that step. The shortest timestep possible is 200 ns. Neurons communicate by sending messages (spikes) across the on-chip network. Spikes can carry up to a 32-bit integer payload. For input-output, the chips have 10 Gb/s off-chip IO interfaces.

Consequently, Loihi 2 requires another layer of design considerations for implementing CLP-SNN, while also providing novel advantageous capabilities. Specifically, the programmable neurons of Loihi 2 depart from the hard-coded leaky integrate-and-fire (LIF) neurons of previous-generation Loihi chips and other neuromorphic hardware solutions. The user can write small programs that simulate the inner computation of different types of neurons. Our *novelty detection*, *modulator*, and *prototype* neurons are designed in this framework. *Novelty detection* neuron identifies novel inputs using a timer-based mechanism mimicking dendritic integration and coincidence detection observed in biological neurons. *Modulator* neuron relays feedback signals and facilitates prototype allocation and adaptation by converting external or internal feedback into third-factor modulatory spikes. The prototype neurons integrate inputs from multiple sources (input, modulator, and other prototype neurons) via distinct dendritic branches and participate in winner-take-all competition through lateral inhibitory connections. We also use the capability of overwriting pre-synaptic traces with graded input spike values, to make the input feature values accessible to the learning engine to update the weights. Overall, the architecture of the CLP-SNN network on Loihi 2 is similar to the SNN

we described in Fig. 2, with slight differences. For example, as the actual label input comes from outside of the chip, we put the match-mismatch circuitry at the CPU as a Python code and only send the scalar feedback signal to the chip and thereafter to the prototype population.

Programmable Neuron Models: In all three of our complex neuron models, dendritic computation-like mechanisms play a central role. The *novelty detection* neuron receives spikes from the input population, triggering an internal timer that spans t_{wait} time steps. If a spike from the prototype population arrives at the other dendrite of the *novelty detection* during this time window, the neuron is reset, preventing it from spiking. However, if no such prototype neuron spike arrives in the t_{wait} time steps, then *novelty detection* neuron spikes to signal the novelty of the input. This mechanism ensures that the neuron only responds to truly novel inputs. The internal timer and reset process can be interpreted as a functional implementation of dendritic integration and coincidence detection, as observed in cortical pyramidal neurons [47, 22]. Specifically, in brain excitatory inputs to one dendritic branch initiate a depolarizing event that primes the neuron to spike after a delay, while inhibitory inputs to other branches within the integration window can suppress or cancel the spiking response.

The *modulator* neuron serves as a relay for feedback signals converging on the prototype population. It receives excitatory input from the novelty detection neuron and converts this signal into a third-factor modulatory spike, facilitating the allocation of a new prototype neuron. Additionally, the modulator neuron receives external feedback signals, such as those from the environment or a supervisory system, translating them into third-factor signals to guide adaptation. As a result, this neuron fulfills two key roles: allocating new prototypes and adapting existing ones.

Finally, the prototype neurons have the most complex neuron model, with several internal variables and dendritic branches, similar to the pyramidal neurons in the brain, which integrate inputs at multiple dendritic segments. It receives input at its three dendritic branches from three populations of neurons: the input neurons, the modulator neurons, and the prototype population itself. Input neurons provide the feedforward input to the (proximal dendrites of) prototype population. The integer-valued or graded spikes of Loihi 2 replace the rate-coding binary spike trains to achieve more efficient communication. Namely, each neuron of the *feature neuron* population can synchronously eject an element of the feature vector, which then all together arrive at the *prototype* neuron's first dendritic branch. The modulator neuron delivers feedback input to the second (distal) dendritic branch of the prototypes. Finally, recursive inhibitory connections facilitate winner-take-all (WTA) competition via targeting the third dendritic branch.

Designing On-chip Learning Rule: Loihi 2's hardware-level learning acceleration allows pro-

grammable learning rules for synaptic variables, enabling activity-dependent synaptic updates. These rules are programmed as sum-of-product equations, where products are composed of dynamic traces and synaptic variables. There are three synaptic variables per synapse: Weight, Delay, and Tag. Each synapse also has access to 2 pre-synaptic and 3 post-synaptic activity traces that are variables storing memory of previous neuron activity. Additionally, the evaluation of every product in the learning rule can be gated by a pre- or post-synaptic gating variable. Traces can be generated by exponential filtering of the pre-synaptic and post-synaptic spike trains or assigned directly in microcode neuron programs. Synaptic weights are updated in parallel across cores during a learning phase, which occurs at programmable intervals.

With these features, the learning engine of Loihi 2 supports distributed and local learning in neural networks. Loihi 2 combines two types of learning locality: on the hardware level with near-memory computing, where the computing logic that updates the weights is next to fast SRAM memory, and on an algorithmic level with the locality of learning, where information required for synaptic update is local to the neurocore. This enables extremely fast and energy-efficient learning compared to methods that require global information, such as back-propagation, by reducing the data movement required during learning. Additionally, Loihi 2 implements event-driven learning, where learning is gated by pre-synaptic spikes, meaning that the weight update may be skipped and most of the learning computation is avoided if no spike is emitted by the pre-synaptic neuron.

The CLP-SNN learning rule (equation (3)) is implemented on Loihi 2 as follows:

$$\Delta w_{ij}(t) = \alpha_i(t) s_i^r(t) (x_j(t) - w_{ij}(t) y_i(t)), \quad (6)$$

where at SNN time step t $\Delta w_{ij}(t)$ is the weight change applied to the synapse between pre-synaptic neuron j and post-synaptic neuron i . Then respectively, $\alpha_i(t)$ is the adaptive learning rate, $y_i(t)$ is the post-synaptic trace, $s_i^r(t)$ is the reward (i.e. third-factor) spike train arriving at the post-synaptic neuron i , while $x_j(t)$ is the pre-synaptic trace of neuron j . Note that t here is SNN time step, not the algorithmic time step as in previous equations. These involve the neuron dynamics over time, which were previously abstracted into a single algorithmic time step. The different spike trains can be written as follows:

$$s_i^m(t) = \sum_m a_i^m \delta(t - t_i^m). \quad (7)$$

Here we use the sum of Dirac delta functions, while t_m s are spike times, $m \in "x", "y", "r"$ denotes the types of different (pre-synaptic, post-synaptic and third factor) spike trains, and a_i^m is the amplitude of the m^{th} spikes for neuron i . Accordingly, we can write the update equations for pre- and post-synaptic traces as follows:

$$x_j(t+1) = \begin{cases} s_j^x(t) & \text{if } \max_j s_j^x(t) > 0, \\ x_j(t) & \text{if } \max_j s_j^x(t) = 0. \end{cases} \quad (8)$$

$$y_i(t+1) = \begin{cases} \sum_j w_{ij} x_j & \text{if } \max_j s_j^x(t) > 0, \\ y_i(t) & \text{if } \max_j s_j^x(t) = 0. \end{cases} \quad (9)$$

Here $\max_j s_j^x(t) > 0$ checks if there is spike arriving from any pre-synaptic neuron, meaning if an input pattern is injected. When this occurs, pre-synaptic traces are updated to the spike amplitudes and kept same till the next pattern. Similarly, post-synaptic traces are updated to the accumulated activation ($\sum_j w_{ij} x_j$), which is effectively dot product between input pattern and the incoming weight vector of that post-synaptic neuron. These traces stay constant till new pattern injection. Finally, the learning rate (i.e. the plasticity) and the goodness score of a specific post-synaptic neuron are updated when a third-factor signal arrives at this neuron.

$$g_i(t+1) = \begin{cases} g_i(t) + s_i^r(t) & \text{if } s_i^r(t) > 0, \\ g_i(t) & \text{if } s_i^r(t) = 0. \end{cases} \quad (10)$$

$$\alpha_i(t+1) = \begin{cases} 1/g_i(t) & \text{if } s_i^r(t) > 0, \\ \alpha_i(t) & \text{if } s_i^r(t) = 0. \end{cases} \quad (11)$$

Experimental Framework

Dataset and Preprocessing: For all experiments, we used the OpenLORIS dataset [44]. The dataset includes 36 video clips for each of 121 objects, which are divided into 40 object categories. We use the category-level labels. We took the first 60 frames from each video clip to remove the imbalance between classes, as video clips have variable lengths. We leverage the off-the-shelf ImageNet-trained EfficientNet-B0 model as the static feature extractor, which is widely used for edge devices [15]. The feature extraction is followed by the L2 normalization of feature vectors. The optimization and comparison of the feature extractors are beyond the scope of this paper.

For both 1-shot and 25-shot learning, each shot corresponds to a collection of one random video clip for each of 40 object classes. For both setups, we did three random seed experiments, meaning the order of the classes and the video clip choices is randomized for each trial.

Baseline Methods: We employed Streaming Linear Discriminant Analysis (SLDA), Nearest Class Mean (NCM), Fine-tuning, Fine-tuning with replay, and Perceptron as baseline methods, similar to the previous work [15, 13]. SLDA is the stream learning version of the well-known linear discriminant analysis (LDA) algorithm [14]. It also uses dot product similarity, while existing implementations did not employ normalization.

We adopted L2 normalization for all methods except Replay, as it was failing with normalized feature vectors. NCM is a basic prototype-based algorithm that keeps one running average prototype for each class, and finds the nearest class mean (e.g., Euclidean distance) for each test sample to make a prediction. Fine-tuning and Perceptron are non-CL baselines, updating weights of the last layers in an online fashion. Fine-tuning with replay stores a specified number of samples for each class, and replays them together with the current sample to mitigate catastrophic forgetting.

Cross-plafrom Latency and energy benchmarking

We achieve cross-Platform comparison consistency, (1) by using the same feature vectors extracted by the same off-the-shelf model across all methods, (2) identical evaluation protocols and metrics, (3) synchronized random seeds for reproducibility. All baseline methods were benchmarked for energy consumption and latency on an NVIDIA Jetson Orin Nano (8GB, 15W TDP) running JetPack 6.2 with PyTorch 2.4.0. This platform was selected as a representative AI edge device comparable to Loihi for on-device computing applications. Energy measurements captured total system power consumption (VDD_IN) using the Tegrastats monitoring tool. Performance metrics were collected by alternating between GPU and CPU execution modes to comprehensively evaluate each method’s computational requirements across both processing units. In contrast, CLP-SNN performance on Loihi 2 was evaluated using an Oheo Gulch system equipped with N3C2-revision Loihi 2 chips. The implementation leveraged Lava 0.11.0.dev0, Lava-Loihi 0.6.0.dev0, and NxCore 2.5.8 software frameworks. For consistency across all platforms, IO latencies were excluded from GPU, CPU, and Loihi 2 benchmark measurements.

With respect to our power nomenclature, the total power consumed by computing hardware comprises two components: static and dynamic power. Static power represents the baseline consumption when the system is idle, including leakage currents and always-on components. Dynamic power refers to the additional consumption during active computation, which includes system workloads and memory accesses.

We performed all characterization experiments with the input dimensionality of 1280, which is the penultimate layer size of the EfficientNet-B0 backbone. The number of classes is set to 40 for all methods. The number of prototypes pre-allocated for both CLP and CLP-SNN is set to 300, as the maximum required prototypes for our experiments. On Loihi 2, CLP-SNN with this network size (1280×300) requires 41 cores out of 128 in a single chip.

References

- [1] Wickliffe C Abraham. Metaplasticity: tuning synapses and networks for plasticity. *Nature Reviews Neuroscience*, 9(5):387–387, 2008.
- [2] Shivam Aggarwal, Kuluhan Binici, and Tulika Mitra. Chameleon: Dual memory replay for online continual learning on edge devices. *IEEE Transactions on Computer-Aided Design of Integrated Circuits and Systems*, 43(6):1663–1676, 2023.
- [3] James B Aimone, Janet Wiles, and Fred H Gage. Computational influence of adult neurogenesis on memory encoding. *Neuron*, 61(2):187–202, 2009.
- [4] Marcus K Benna and Stefano Fusi. Computational principles of synaptic memory consolidation. *Nature neuroscience*, 19(12):1697–1706, 2016.
- [5] Seyed Amir Bidaki, Amir Mohammadkhah, Kiyan Rezaee, Faeze Hassani, Sadegh Eskandari, Maziar Salahi, and Mohammad M Ghassemi. Online continual learning: A systematic literature review of approaches, challenges, and benchmarks. *arXiv preprint arXiv:2501.04897*, 2025.
- [6] Dan Bohus, Sean Andrist, Ashley Feniello, Nick Saw, and Eric Horvitz. Continual learning about objects in the wild: An interactive approach. In *Proceedings of the 2022 International Conference on Multimodal Interaction*, pages 476–486, 2022.
- [7] Tom Brown, Benjamin Mann, Nick Ryder, Melanie Subbiah, Jared D Kaplan, Prafulla Dhariwal, Arvind Neelakantan, Pranav Shyam, Girish Sastry, Amanda Askell, et al. Language models are few-shot learners. *Advances in neural information processing systems*, 33:1877–1901, 2020.
- [8] Mike Davies, Narayan Srinivasa, Tsung Han Lin, Gautham Chinya, Yongqiang Cao, Sri Harsha Choday, Georgios Dimou, Prasad Joshi, Nabil Imam, Shweta Jain, Yuyun Liao, Chit Kwan Lin, Andrew Lines, Ruokun Liu, Deepak Mathai, Steven McCoy, Arnab Paul, Jonathan Tse, Gurukanthan Venkataraman, Yi Hsin Weng, Andreas Wild, Yoonseok Yang, and Hong Wang. Loihi: A neuromorphic manycore processor with on-chip learning. *IEEE Micro*, 38:82–99, 2018.
- [9] Mike Davies, Andreas Wild, Garrick Orchard, Yulia Sandamirskaya, Gabriel A Fonseca Guerra, Prasad Joshi, Philipp Plank, and Sumedh R Risbud. Advancing neuromorphic computing with loihi: A survey of results and outlook. *Proceedings of the IEEE*, 109(5):911–934, 2021.
- [10] Graham Findlay, Giulio Tononi, and Chiara Cirelli. The evolving view of replay and its functions in wake and sleep. *Sleep Advances*, 1(1):zpab002, 2020.
- [11] Wulfram Gerstner, Werner M Kistler, Richard Naud, and Liam Paninski. *Neuronal dynamics: From single neurons to networks and models of cognition*. Cambridge University Press, 2014.
- [12] Elvin Hajizada, Patrick Berggold, Massimiliano Iacono, Arren Glover, and Yulia Sandamirskaya. Interactive continual learning for robots: a neuromorphic approach. In *Proceedings of the International Conference on Neuromorphic Systems 2022*, pages 1–10, 2022.
- [13] Elvin Hajizada, Balachandran Swaminathan, and Yulia Sandamirskaya. Continual learning for autonomous robots: A prototype-based approach. In *2024 IEEE/RSJ International Conference on Intelligent Robots and Systems (IROS)*, pages 13988–13995, 2024.
- [14] Tyler L Hayes and Christopher Kanan. Life-long machine learning with deep streaming linear discriminant analysis. In *Proceedings of the IEEE/CVF conference on computer vision and pattern recognition workshops*, pages 220–221, 2020.
- [15] Tyler L Hayes and Christopher Kanan. Online continual learning for embedded devices. *arXiv preprint arXiv:2203.10681*, 2022.
- [16] Donald Olding Hebb. *The organization of behavior: A neuropsychological theory*. Psychology press, 2005.
- [17] Shaoyi Huang, Haowen Fang, Kaleel Mahmood, Bowen Lei, Nuo Xu, Bin Lei, Yue Sun, Dongkuan Xu, Wujie Wen, and Caiwen Ding. Neurogenesis dynamics-inspired spiking neural network training acceleration. In *2023 60th ACM/IEEE Design Automation Conference (DAC)*, pages 1–6. IEEE, 2023.
- [18] Marta Huelin Gorri, Masahiro Takigawa, and Daniel Bendor. The role of experience in prioritizing hippocampal replay. *Nature Communications*, 14(1):8157, 2023.
- [19] Nabil Imam and Thomas A Cleland. Rapid online learning and robust recall in a neuromorphic olfactory circuit. *Nature Machine Intelligence*, 2(3):181–191, 2020.
- [20] Intel Corporation. Lava: A software framework for neuromorphic computing, 2021. Accessed: [Date].
- [21] Jeffry S Isaacson and Massimo Scanziani. How inhibition shapes cortical activity. *Neuron*, 72(2):231–243, 2011.
- [22] Jeffry S Isaacson and Massimo Scanziani. How inhibition shapes cortical activity. *Neuron*, 72(2):231–243, 2011.

[23] Mohsen Jafarzadeh, Akshay Raj Dhamija, Steve Cruz, Chunchun Li, Touqeer Ahmad, and Terrence E Boult. A review of open-world learning and steps toward open-world learning without labels. *arXiv preprint arXiv:2011.12906*, 2020.

[24] KJ Joseph, Salman Khan, Fahad Shahbaz Khan, and Vineeth N Balasubramanian. Towards open world object detection. In *Proceedings of the IEEE/CVF conference on computer vision and pattern recognition*, pages 5830–5840, 2021.

[25] Aymen Rayane Khouas, Mohamed Reda Bouadjenek, Hakim Hacid, and Sunil Aryal. Training machine learning models at the edge: A survey. *arXiv preprint arXiv:2403.02619*, 2024.

[26] Dongwan Kim and Bohyung Han. On the stability-plasticity dilemma of class-incremental learning. In *Proceedings of the IEEE/CVF Conference on Computer Vision and Pattern Recognition*, pages 20196–20204, 2023.

[27] Dhireesha Kudithipudi, Mario Aguilar-Simon, Jonathan Babb, Maxim Bazhenov, Douglas Blackiston, Josh Bongard, Andrew P Brna, Suraj Chakravarthi Raja, Nick Cheney, Jeff Clune, et al. Biological underpinnings for lifelong learning machines. *Nature Machine Intelligence*, 4(3):196–210, 2022.

[28] Navjot Kukreja, Alena Shilova, Olivier Beaumont, Jan Huckleheim, Nicola Ferrier, Paul Hovland, and Gerard Gorman. Training on the edge: The why and the how. In *2019 IEEE International Parallel and Distributed Processing Symposium Workshops (IPDPSW)*, pages 899–903. IEEE, 2019.

[29] Dawei Li, Serafettin Tasci, Shalini Ghosh, Jingwen Zhu, Junting Zhang, and Larry Heck. Rilod: Near real-time incremental learning for object detection at the edge. In *Proceedings of the 4th ACM/IEEE Symposium on Edge Computing*, pages 113–126, 2019.

[30] Timothy P Lillicrap, Adam Santoro, Luke Marris, Colin J Akerman, and Geoffrey Hinton. Backpropagation and the brain. *Nature Reviews Neuroscience*, 21(6):335–346, 2020.

[31] Ji Lin, Ligeng Zhu, Wei-Ming Chen, Wei-Chen Wang, Chuang Gan, and Song Han. On-device training under 256kb memory. *Advances in Neural Information Processing Systems*, 35:22941–22954, 2022.

[32] Michael McCloskey and Neal J Cohen. Catastrophic interference in connectionist networks: The sequential learning problem. In *Psychology of learning and motivation*, volume 24, pages 109–165. Elsevier, 1989.

[33] Mishal Fatima Minhas, Rachmad Vidya Wicaksana Putra, Falah Awwad, Osman Hasan, and Muhammad Shafique. Continual learning with neuromorphic computing: Theories, methods, and applications. *arXiv preprint arXiv:2410.09218*, 2024.

[34] Richa Mishra and Manan Suri. A survey and perspective on neuromorphic continual learning systems. *Frontiers in Neuroscience*, 17:1149410, 2023.

[35] Erkki Oja. Simplified neuron model as a principal component analyzer. *Journal of mathematical biology*, 15:267–273, 1982.

[36] Garrick Orchard, E Paxton Frady, Daniel Ben Dayan Rubin, Sophia Sanborn, Sumit Bam Shrestha, Friedrich T Sommer, and Mike Davies. Efficient neuromorphic signal processing with loihi 2. In *2021 IEEE Workshop on Signal Processing Systems (SiPS)*, pages 254–259. IEEE, 2021.

[37] Andrei Paleyes, Raoul-Gabriel Urma, and Neil D Lawrence. Challenges in deploying machine learning: a survey of case studies. *ACM computing surveys*, 55(6):1–29, 2022.

[38] Lorenzo Pellegrini, Vincenzo Lomonaco, Gabriele Graffieti, and Davide Maltoni. Continual learning at the edge: Real-time training on smartphone devices. *arXiv preprint arXiv:2105.13127*, 2021.

[39] Vijay Janapa Reddi. Mlsysbook.ai: Principles and practices of machine learning systems engineering. In *2024 International Conference on Hardware/Software Codesign and System Synthesis (CODES+ ISSS)*, pages 41–42. IEEE, 2024.

[40] Haoyu Ren, Darko Anicic, and Thomas A Runkler. Tinyol: Tinyml with online-learning on microcontrollers. In *2021 international joint conference on neural networks (IJCNN)*, pages 1–8. IEEE, 2021.

[41] Mengye Ren, Michael L Iuzzolino, Michael C Mozer, and Richard S Zemel. Wandering within a world: Online contextualized few-shot learning. *arXiv preprint arXiv:2007.04546*, 2020.

[42] Catherine D Schuman, Shruti R Kulkarni, Maryam Parsa, J Parker Mitchell, Prasanna Date, and Bill Kay. Opportunities for neuromorphic computing algorithms and applications. *Nature Computational Science*, 2(1):10–19, 2022.

[43] Khadija Shaheen, Muhammad Abdullah Hanif, Osman Hasan, and Muhammad Shafique. Continual learning for real-world autonomous systems: Algorithms, challenges and frameworks. *Journal of Intelligent & Robotic Systems*, 105(1):9, 2022.

[44] Qi She, Fan Feng, Xinyue Hao, Qihan Yang, Chuanlin Lan, Vincenzo Lomonaco, Xuesong Shi,

Zhengwei Wang, Yao Guo, Yimin Zhang, et al. Openloris-object: A robotic vision dataset and benchmark for lifelong deep learning. In *2020 IEEE international conference on robotics and automation (ICRA)*, pages 4767–4773. IEEE, 2020.

[45] Sumit Bam Shrestha, Jonathan Timcheck, Paxon Frady, Leobardo Campos-Macias, and Mike Davies. Efficient video and audio processing with loihi 2. In *ICASSP 2024-2024 IEEE International Conference on Acoustics, Speech and Signal Processing (ICASSP)*, pages 13481–13485. IEEE, 2024.

[46] Kenneth Stewart, Garrick Orchard, Sumit Bam Shrestha, and Emre Neftci. Online few-shot gesture learning on a neuromorphic processor. *IEEE Journal on Emerging and Selected Topics in Circuits and Systems*, 10(4):512–521, 2020.

[47] Greg J Stuart and Nelson Spruston. Dendritic integration: 60 years of progress. *Nature neuroscience*, 18(12):1713–1721, 2015.

[48] Yonatan Sverdlov and Shimon Ullman. Efficient rehearsal free zero forgetting continual learning using adaptive weight modulation. *arXiv preprint arXiv:2311.15276*, 2023.

[49] Rohan Taori, Achal Dave, Vaishaal Shankar, Nicholas Carlini, Benjamin Recht, and Ludwig Schmidt. Measuring robustness to natural distribution shifts in image classification. *Advances in Neural Information Processing Systems*, 33:18583–18599, 2020.

[50] Daniel Vela, Andrew Sharp, Richard Zhang, Trang Nguyen, An Hoang, and Oleg S Pianykh. Temporal quality degradation in ai models. *Scientific Reports*, 12(1):11654, 2022.

[51] Eli Verwimp, Matthias De Lange, and Tinne Tuytelaars. Rehearsal revealed: The limits and merits of revisiting samples in continual learning. In *Proceedings of the IEEE/CVF International Conference on Computer Vision*, pages 9385–9394, 2021.

[52] Jianren Wang, Xin Wang, Yue Shang-Guan, and Abhinav Gupta. Wanderlust: Online continual object detection in the real world. In *Proceedings of the IEEE/CVF international conference on computer vision*, pages 10829–10838, 2021.

[53] Qiuyan Xiang, Lingling Zi, Xin Cong, and Yan Wang. Concept drift adaptation methods under the deep learning framework: A literature review. *Applied Sciences*, 13(11):6515, 2023.

[54] Kashu Yamazaki, Viet-Khoa Vo-Ho, Darshan Bulsara, and Ngan Le. Spiking neural networks and their applications: A review. *Brain sciences*, 12(7):863, 2022.

[55] Liheng Yuan, Heng Li, Beihao Xia, Cuiying Gao, Mingyue Liu, Wei Yuan, and Xinge You. Recent advances in concept drift adaptation methods for deep learning. In *IJCAI*, pages 5654–5661, 2022.